https://dx.doi.org/10.1016/j.eswa.2023.121478



# Surface quality prediction and quantitative evaluation of process parameter effects for 3D printing with transfer learning-enhanced gradient-boosting decision trees

Jianjian Zhu [a, b, *], Zhongqing Su [a, b], Qingqing Wang [a, c], Zifeng Lan [d], Frankie Siu-fai Chan [e], Zhibin Han [f], Zhaokun Wang [a], Sidney Wing-fai Wong [e], Andy Chi-fung Ngan[e]

[a] *Department of Mechanical Engineering, The Hong Kong Polytechnic University, Kowloon, Hong Kong S.A.R.*

[b] *The Hong Kong Polytechnic University Shenzhen Research Institute, Shenzhen 518057, P.R. China*

[c] *School of System Design and Intelligent Manufacturing, Southern University of Science and Technology, Shenzhen, 518055, P.R. China*

[d] *School of Engineering, The University of Tokyo, Tokyo, Japan*

[e] *Industrial Center, The Hong Kong Polytechnic University, Kowloon, Hong Kong S.A.R.*

[f] *Department of Mechanical and Automation Engineering, The Chinese University of Hong Kong, Hong Kong S.A.R.*

[*] Corresponding Author: Dr. Jianjian Zhu, Email: zhujj.work@outlook.com

Co-author's Email Address: Zhongqing Su: zhongqing.su@polyu.edu.hk, Qingqing Wang: qingqing57.wang@connect.polyu.hk, Zifeng Lan: lanzf@iis.u-tokyo.ac.jp, Frankie Siu-fai Chan: frankie.sf.chan@polyu.edu.hk, Zhibin Han: zhibinhan@link.cuhk.edu.hk, Zhaokun Wang: zhaokun.wang@connect.polyu.hk, Sidney Wing-fai Wong: sidney.wong@polyu.edu.hk, Andy Chi-fung Ngan: chi-fung-habi.ngan@polyu.edu.hk

**Abstract**

3D printing has the potential to revolutionize industrial manufacturing through efficient and sustainable techniques. Fused Deposition Modeling (FDM) is a broadly deployed technique among various 3D printing methods. However, the surface quality of FDM is greatly influenced by multiple factors, making it challenging to unravel the relationship between printing quality and parameter settings. To break through this bottleneck, this study proposes an intelligent approach that combines Transfer Learning (TL)-based Feature Extractor (FE) and Gradient-Boosting Decision Trees (GBDT) to investigate the effects of FDM printing parameters on surface quality. Experiments are conducted in the laboratory to validate the effectiveness of the FE-GBDT, which is then compared with the exemplary Machine Learning (ML) algorithms. The results show that our proposed TL model can achieve high precision and accuracy over 0.9900, demonstrating the efficacy of FE-GBDT in deciphering the impact of FDM printing parameters on surface quality. The contribution of each parameter is evaluated and indicates that layer height could dramatically affect the surface quality with an importance score of 0.626. The results provide valuable insights for the 3D printing community, proving that the FE-GBDT approach offers improved generalization, faster training, enhanced feature extraction, addressing data scarcity, and the ability to leverage the strengths of both approaches for superior performance across various tasks.

**Keywords**

3D printing, fused deposition modeling, process parameters, surface quality, transfer learning, gradient-boosting decision trees.

## 1. Introduction

3D printing, also known as Additive Manufacturing (AM), is a revolutionary technology with significant implications for industrial sectors due to its potential to provide highly efficient and sustainable manufacturing techniques (Jindal et al., 2021). Fused Deposition Modeling (FDM) is a widely used 3D printing method among these techniques, which is implemented by melting and extruding thermoplastic filaments layer-by-layer to create stereo objects (N. Li et al., 2019). The surface quality of 3D-printed products plays a vital role in their performance and durability. Poor surface quality could cause adverse impacts on product performance, such as aesthetics and production costs. Therefore, investigating process parameters on the surface quality is significant for quality assessment, process optimization, and application adaptability in the 3D printing community, where surface quality can be significantly impacted by several factors, such as scanning strategy, extrusion speed, layer thickness, temperature, and material flow (Ngo et al., 2018). Accordingly, the configuration of process parameters directly influences surface quality and structural performance, which are actual bottlenecks and challenges in practical applications (Pérez et al., 2018).

To break through the bottleneck above, researchers and industrial professionals made substantial efforts to improve various properties of FDM-printed products. These efforts include investigating the effects of process parameters on surface roughness and structural performance (Altan et al., 2018; Charalampous et al., 2022), achieving a balance between mechanical properties, surface finish quality, and building time (Kam et al., 2023; Yang et al., 2019), improving the surface quality of micro-sized near-net-

shaped components (Rajamani et al., 2022), exploring the influence of printing parameters on surface finish using response surface method (Radhwan et al., 2019). Besides, some researchers are focused on reviewing studies of statistics and the design of experiments for enhancing mechanical properties, building time, and part quality (Jaisingh Sheoran & Kumar, 2020) alongside FDM process parameter optimization (Dey & Yodo, 2019).

Although existing studies have explored the surface quality concerns of the FDM process, quantitatively evaluating 3D printing parameters and calculating the contributions of each parameter to surface quality with conventional statistical methods remains a significant challenge. To break through this bottleneck, various approaches integrating the printing process with Neural Networks (NN) and Machine Learning (ML) have been developed. Back-Propagation Neural Networks (BPNN), Decision Trees (DT), Random Forests (RF), Support Vector Regression (SVR), and Ridge Regression (RR) are among the commonly used NN and ML methods in previous studies (Barrios & Romero, 2019; Boschetto et al., 2013; Cerro et al., 2021; Hooda et al., 2021; Z. Li et al., 2019; Wu et al., 2019). Additionally, Deep Learning (DL) methods like Convolutional Neural Networks (CNN) have been employed to predict the surface quality of FDM-printed products (Jin et al., 2019; J. Zhang et al., 2019). However, regarding industrial circumstances, traditional ML and DL methods usually have poor generalization abilities, hindering their more comprehensive application. With the rapid advancement of Artificial Intelligence (AI), Transfer Learning (TL) has emerged as a prospective solution to improve the generalization capabilities of various intelligent

models while lowering the dataset requirements (Zhuang et al., 2021). TL leverages knowledge gained from one or multiple source domains to enhance the overall performance of a reused model in a target domain (Tan et al., 2018; Weiss et al., 2016). Thus, it provides a potential remedy to overcome the challenges regarding quantitatively evaluating the surface quality of 3D-printed products.

To promote the resolution of the present hindrance, we proposed an intelligent approach to quantitatively investigate the effects of 3D printing process parameters on surface quality regarding the features obtained by a TL-based Feature Extractor (FE). In this study, surface quality is represented by surface roughness. Specifically, the FE is a CNN with one dimension (1DCNN) in this study, pre-trained by the prior data collected from other cases, yet with the classifier removed. Then it is redeployed using the TL strategy to obtain the bottleneck features from the data of the new scenarios. The Gradient-Boosting Decision Trees (GBDT) classifier is attached to the FE to perform the classification tasks using the FE-exported features. Therefore, the proposed intelligent approach is named FE-GBDT herein. The proposed FE-GBDT offers improved generalization by leveraging knowledge from pre-trained models, faster training through well-initialized parameters, and enhanced feature extraction capturing complex patterns. It also addresses data scarcity by utilizing knowledge from similar scenarios while combining the strengths of both approaches to achieve superior performance on various tasks. The main research objective of this study is to investigate the impact of FDM parameters on surface quality using intelligent methods and to quantify the contribution of each parameter to the surface quality of 3D-printed

products by employing the proposed FE-GBDT approach.

The main novelty of the proposed FE-GBDT approach is that it can achieve high accuracy on the new dataset based on the previous dataset from other similar scenarios, which promotes lowering the data quantity and quality requirement. By combining these two approaches, we can also integrate the feature representation of pre-trained models with the ensemble learning of GBDT, fully leveraging their respective advantages to improve the performance and generalization capability of the model. The findings of this study provide evidence supporting the effectiveness of the proposed TL-based FE-GBDT approach in quantitatively evaluating the effects of 3D printing parameters on surface quality and their corresponding contributions.

The organization of this paper is as follows: Section 2 describes the fundamental of the FE-GBDT and its relevant algorithms, followed by the experimental configuration and dataset construction in Section 3. Section 4 presents the experimental results and the relevant discussion, as well as the detailed analyses. Lastly, Section 5 concludes the critical findings of the study and provides the avenue for subsequent work.

## 2. Principles and methods

### *2.1. Theoretical principles*

#### *2.1.1. Fundamental of TL and 1DCNN*

The TL applies knowledge and expertise from addressing one problem to another related one. The principle of TL states that a model trained on a large and diverse dataset

can serve as a pre-trained model for another new dataset, resulting in improved performance indicators (Tan et al., 2018; Weiss et al., 2016; Zhuang et al., 2021). The pre-trained model has acquired beneficial features that can be employed to enhance the performance of the new model. By reusing these specific features, the new performance of the rebuilt model can be improved with an accelerated learning process using fewer training examples (Agarwal et al., 2021). To provide a better understanding of TL principle, a schematic diagram is presented in Fig. 1.

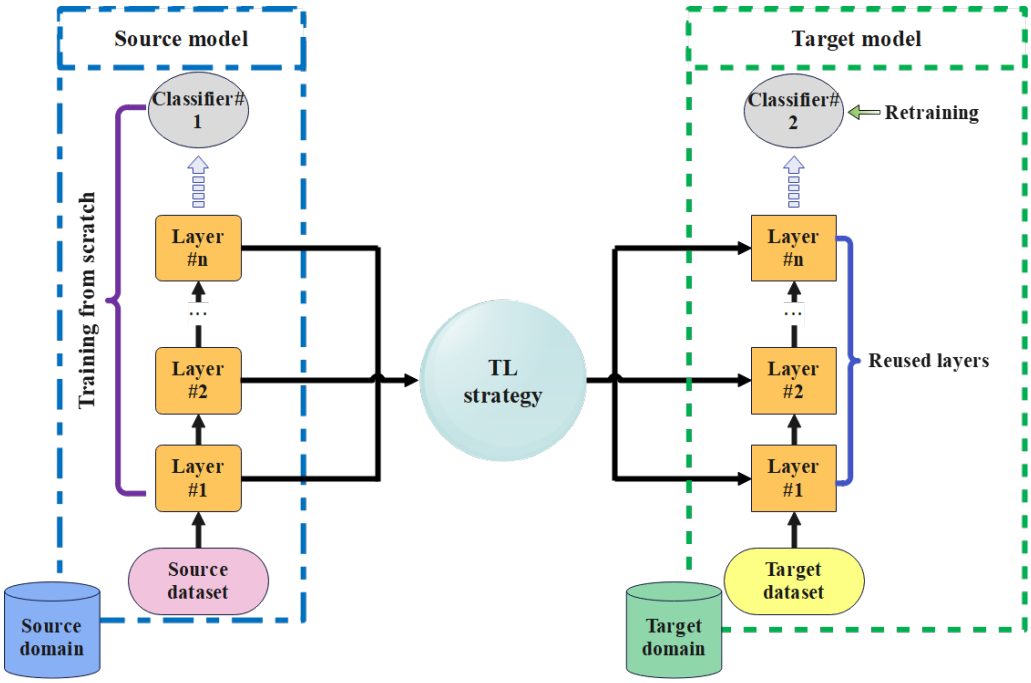


**Fig. 1.** Workflow of the TL strategy.

Supposing the domain $D$ contains two constituents, feature space $\dot{X}$ and marginal probability distribution function $P(X)$, where $X = \{x_1, x_2, \ldots, x_n\} \in \dot{X}$. For a given particular domain, we can consider $D = \{\dot{X}, P(X)\}$. A task also includes two constituents, a label space $\dot{Y}$ and an objective predictive function $f(\cdot)$, *i.e.*, task $T$ is

represented by $T = \{\dot{Y}, f(\cdot)\}$ (Agarwal et al., 2021). In this study, the domain is defined as a pair $D = \{\dot{X}, P(X)\}$, where $D_S \neq D_T$ implies that either $\dot{X}_S \neq \dot{X}_T$ or $P_S(X) \neq P_T(X)$. Specifically, the feature space involved in this study consists of FDM-based 3D printing parameters, while the labels are represented with surface quality.

The 1DCNN model comprises multiple components, including the layers for input, convolutional operation, pooling operation, dropout, and classification. Collectively, these layers are employed to identify pertinent characteristics of input data and allocate them into distinct categories. The primary architecture of 1DCNN mentioned in this study includes one classifier, four convolutional layers, one max-pooling layer, and one dropout layer, as presented in Fig. 2. The convolutional and pooling layers are deployed to extract features from data sequences and reduce their dimensions. A dropout layer is adopted to prevent overfitting, while the layer for flattening converts bottleneck features into a column vector before being fed into the classifier. Moreover, the blocks of a trained source model will be utilized and repurposed in new application scenarios.

Specifically, integrating 1DCNN and TL is suitable for FDM printing datasets due to the scarcity of labeled data, the potential transfer of domain-specific knowledge, the benefits of parameter initialization and model optimization, and improved model generalization. Through leveraging pre-trained models and their learned features, the TL strategy enables better performance with limited labeled data, enhances understanding of critical features in FDM printing processes, reduces training time, and facilitates adaptation to new samples. Hence, combining the TL strategy with 1DCNN is a potential solution to effectively address challenges in FDM printing datasets.

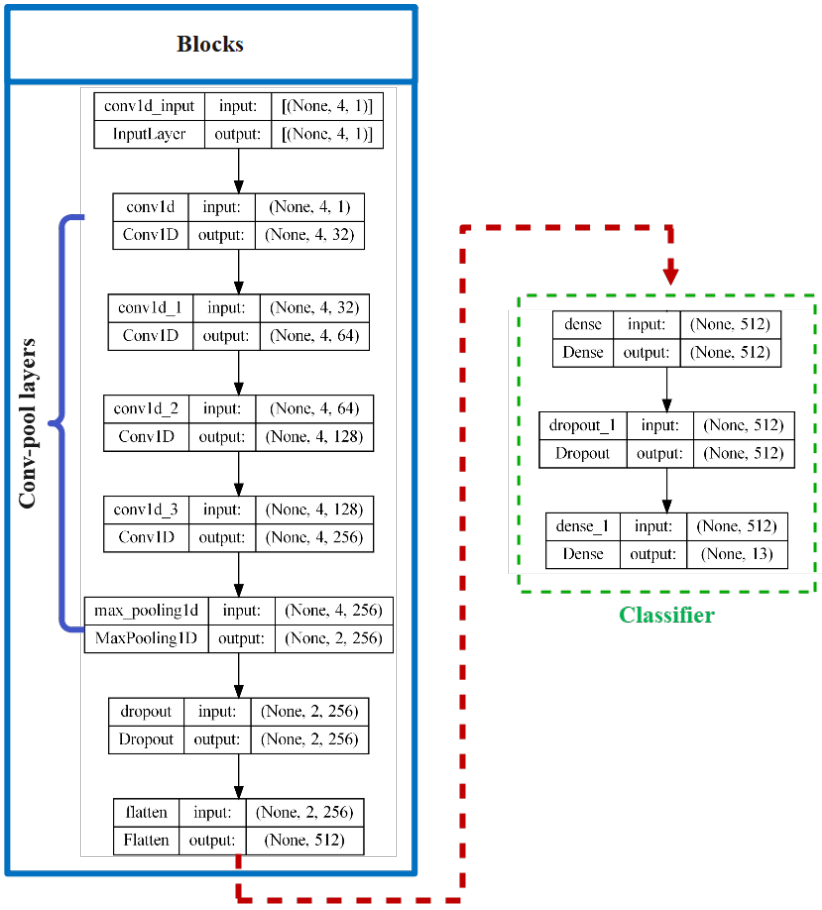


**Fig. 2.** Schematic of 1DCNN model architecture.

### *2.1.2. Fundamental of TL-based FE-GBDT*

The GBDT is the algorithm employing a collection of decision trees to generate predictions. GBDT has gained recognition as one of the robust ML algorithms for multi-task classification due to its high prediction accuracy, capacity to handle multi-class problems, ability to select features, reliability against noise and missing data, and strong interpretability.

In the GBDT algorithm, a sequence of decision trees is added to an ensemble iteratively, whereby each subsequent tree is trained to rectify the shortcomings of its

forerunner. The ultimate prediction is obtained by aggregating the weighted summation of predictions from all the trees (Liang et al., 2020; Z. Zhang & Jung, 2021).

Supposing that $\{x_i, y_i\}_{i=1}^{m}$ represents the sample dataset, where $x_i = (x_{1i}, x_{2i}, \cdots, x_{ri})$ represents indicators, and $y_i$ denotes the labels. Then the specific steps of GBDT are yielded as follows (Liang et al., 2020; Rao et al., 2019):

Step1: The initial constant value $\gamma$ is obtained as:

$$F_0(x) = arg\ \min_{\gamma} \sum_{i=1}^{m} L(y_i, \gamma) \tag{1}$$

where $L(y_i, \gamma)$ is the loss function.

Step2: The residual along the gradient direction is written as:

$$\hat{y}_i = -\left[\frac{\partial L(y_i, F(x_i))}{\partial F(x_i)}\right]_{f(x)=f_{n-1}(x)} \tag{2}$$

where *n* indicates the number of iterations, and *n*=1, 2, 3, …, N.

Step3: The initial model $T(x_i; \alpha_n)$ is obtained by fitting sample data, and the $\alpha_n$ is calculated based on the least square method as:

$$\alpha_n = arg\ \min_{\alpha,\beta} \sum_{i=1}^{m} \left(\hat{y}_i - \beta T(x_i; \alpha)\right)^2 \tag{3}$$

Step4: By minimizing the loss function, the current weight is expressed as:

$$\gamma_n = arg\ \min_{\gamma} \sum_{i=1}^{m} L\left(y_i, F_{n-1}(x) + \gamma T(x_i; \alpha_n)\right) \tag{4}$$

Step5: The model is then updated as follows:

$$F_n(x) = F_{n-1}(x) + \gamma_n T(x_i; \alpha_n) \tag{5}$$

The loop is executed continuously until the convergence conditions or the specified number of iterations are fulfilled.

Based on the principles of TL and GBDT in the above context, the FE-GBDT approach incorporates the advantages of both TL and GBDT in improving the ultimate

performance and generalization capability, as shown in Fig. 3. The layers included in the FE are frozen to prevent the weight values from being updated when reused for extracting specific features in the new scenarios. Then, the GBDT performs the classification tasks based on the output exported from the FE.

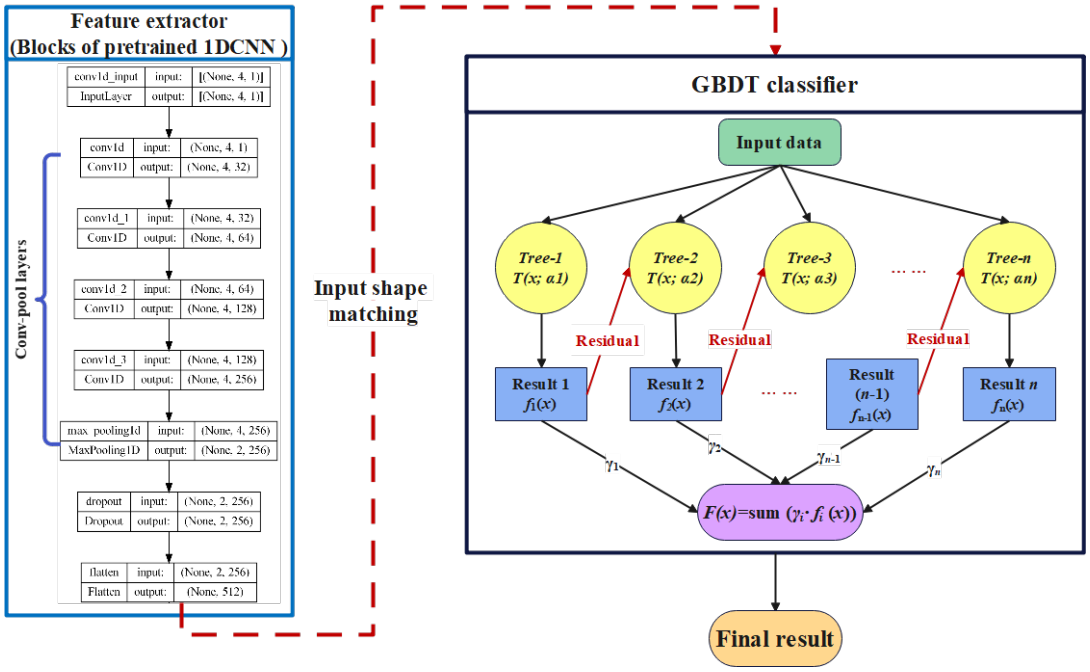


**Fig. 3.** Schematic of FE-GBDT architecture.

## *2.2. Methods for promoting model performance*

### *2.2.1. SMOTE for data imbalance elimination*

The Synthetic Minority Over-sampling TEchnique (SMOTE) is an oversampling method that aims to tackle imbalanced datasets in classification problems, first developed by Chawla *et al.* (Chawla et al., 2002a). Such datasets exhibit a significant

difference between minority and majority classes, leading to suboptimal performance of classifiers. To alleviate this problem, SMOTE generates synthetic instances by interpolating between existing observations of the minority class, which has been proven effective in improving the performance of classifiers on imbalanced datasets (Fernandez et al., 2018). The main advantage of the SMOTE algorithm includes the following aspects: (1) Generating synthetic samples for the minority class, effectively addressing imbalanced datasets, and improving classifier performance; (2) Reducing the risk of overfitting, enhancing the generalization ability of classifiers trained on imbalanced data by increasing the number of minority class samples; (3) Capturing the characteristics and patterns of the minority class, leading to more accurate predictions and a better understanding of the data distribution.

Explicitly, the SMOTE can generate a new synthetic instance by supposing a minority class instance $x_i$ and its $k$ nearest neighbors in the feature space, given by:

$$x_{new} = x_i + \lambda(x_j - x_i) \tag{6}$$

where $x_j$ is a randomly selected nearest neighbor $x_i$, and $\lambda$ is a random value between 0 and 1. This process is repeated for each minority class instance, resulting in a new dataset with a balanced class distribution (Blagus & Lusa, 2013; Chawla et al., 2002b). Then the imbalance of the data among different classes can be effectively eliminated.

*2.2.2. Optimization for FE-GBDT parameters*

The Randomized Search and Cross Validation (RSCV) algorithm is a simple yet effective method for searching the optimal combination of hyperparameters. The

fundamental is to randomly sample hyperparameters from a predetermined distribution and evaluate their performance using a validation set (Andradóttir, 2015). The advantage of random search over other methods like grid search is that it is less computationally expensive, especially in high-dimensional search spaces. Additionally, random search makes no assumptions about the search space structure and is thus more flexible (Andradóttir, 2006).

Generally, supposing $H$ denotes the hyperparameter space, $G(h)$ denotes the distribution of a single hyperparameter $h$ in $H$, and $S$ denotes the number of samples to draw from $H$. Then, the goal of the random search is to find the set of hyperparameters $H^*$ that maximizes the performance metric $P$ on a validation set $V$, subject to the constraint that $H^* \in H$. Mathematically, it can be described as (Andradóttir, 2015; Liashchynskyi & Liashchynskyi, 2019):

$$H^* = argmax_{H_i \in H_S} P(M_i) \tag{7}$$

where $M_i = f(H_i, D_{train})$, $H_s = \{h_1, h_2, ..., h_S\}$, $h_i \sim G(h), \forall h_i \in H_s$. Moreover, $f(\cdot)$ is the function that trains the model with the hyperparameters $H_i$ and training dataset $D_{train}$.

By randomly sampling hyperparameters from $H$ according to the distributions $G(h)$, a set of hyperparameters $H_S$ can be generated to train multiple models $M_i$. The set of hyperparameters with the best validation performance is denoted by $H^*$. A final model can then be implemented by selecting the optimal set of hyperparameters, which have been optimized to achieve superior performance on the testing dataset (Andradóttir, 2015; Liashchynskyi & Liashchynskyi, 2019).

*2.2.3. Quantifying effects of 3D printing parameters*

Feature Importance (FI) is a significant indicator with a scope from 0 to 1.0. It can be calculated by measuring the total reduction of impurity, to which each feature contributes on all decision trees when the GBDT method is adopted. The impurity reduction of a feature is computed by measuring the decrease in the loss function value when a feature is selected as the splitting point for a tree node.

Mathematically, the formula for calculating the FI score regarding the feature $f_i$ is given by Eq. (8):

$$FI(f_i) = \frac{\sum_{t=1}^{T} I(f_{split,t}=f_i)\Delta\text{loss}_t}{\sum_{t=1}^{T} \Delta\text{loss}_t} \tag{8}$$

where $T$ denotes the total number of trees in the GBDT ensemble, and $f_{split,t}$ represents the feature used for splitting at node $t$ of the $t^{th}$ decision tree. The indicator function $I(f_{split,t} = f_i)$ can be described with the following Eq. (9):

$$I(f_{split,t} = f_i) = \begin{cases} 1, & \text{if } f_i \text{ is chosen as the splitting feature at node } t \\ 0, & \text{other} \end{cases} \tag{9}$$

Thus, according to Eqs. (8) and (9), the numerator sums the impurity reduction achieved by all splits that use the feature $f_i$. In Eq. (8), the term $\Delta\text{loss}_t$ represents the decrease in the loss function value due to the split at node $t$. The loss function measures the difference between the predicted and actual values, and the objective of the GBDT algorithm is to minimize this difference. The decrease in loss due to a split can be computed using the following formula:

$$\Delta loss = loss(S_t) - \frac{N_{left}}{N} loss(S_{left}) - \frac{N_{right}}{N} loss(S_{right}) \tag{10}$$

where $loss(S_t)$ represents the loss value for the parent node $t$ before splitting, $S_{left}$

and $S_{right}$ are the subsets of data points obtained by the split; $N_{left}$ and $N_{right}$ are the number of data points in each subset. The fractions $N_{left}/N$ and $N_{right}/N$ represent the proportion of data points allocated to each subset.

Thereby, the FI score measures the contribution of each feature $f_i$ to the overall impurity reduction achieved by the GBDT. It should be noted that the features involved in experiments are 3D printing parameters in this study. Hence the contribution of each 3D printing parameter to surface quality can be effectively evaluated.

## 3. Samples printing and datasets construction

### *3.1. Samples fabrication and testing*

As previously mentioned, the surface quality of products in FDM is significantly influenced by the 3D printing parameters (Radhwan et al., 2019). This study investigates the effects of four specific printing parameters, namely layer height, scan speed, material flow, and nozzle temperature, on the quality of FDM-printed products. The material used in experiments of this study is a filament made of Poly-Lactic Acid (PLA) with a diameter of 1.75 mm. The specific values assigned to each 3D printing parameter can be found in Table 1. The suggested printing values from the supplier for the PLA filament (Ultimaker BV, Netherlands), which is commonly used in our laboratory, are also mentioned in Table 1. Accordingly, there are 625 groups of parameter combinations in total. Each sample is produced using 3D printing, utilizing a unique configuration of process parameters, resulting in the fabrication of 625 individual samples.

The dimensions of printed samples are 10 mm×5 mm×15 mm in length, width, and height, respectively. The printing order is from bottom to top, and each piece has an exclusive number attached to the top face to distinguish it from other samples. Hence, the surface selected for roughness measurement is the side face in terms of the FDM printing sequence. The type of printer used for 3D printing, particularly for the FDM process, is Ultimaker-S5 (Ultimaker BV, Netherlands). The surface roughness of each sample is measured by the surface profilometer (Surftest SJ-210, Mitutoyo, Japan). The surface roughness is obtained with the surface profilometer by testing three times repeatedly on one sample at different locations. The average value is then used for characterizing the surface roughness of this sample, which guarantees the reliability of the measurement. The platform for sample fabrication and surface roughness measurement is presented in Fig. 4.

**Table 1**

3D printing parameters and values employed in experiments.

| Layer height (mm) | Scan speed (mm/s) | Nozzle temp. (°C) | Material flow (%) |
|---|---|---|---|
| Suggested: 0.1-0.3 | Suggested: 60-80 | Suggested: 190-220 | Default: 100 |
| 0.05 | 60 | 195 | 95 |
| 0.10 | 65 | 200 | 100 |
| 0.15 | 70 | 205 | 105 |
| 0.20 | 75 | 210 | 110 |
| 0.25 | 80 | 215 | 115 |

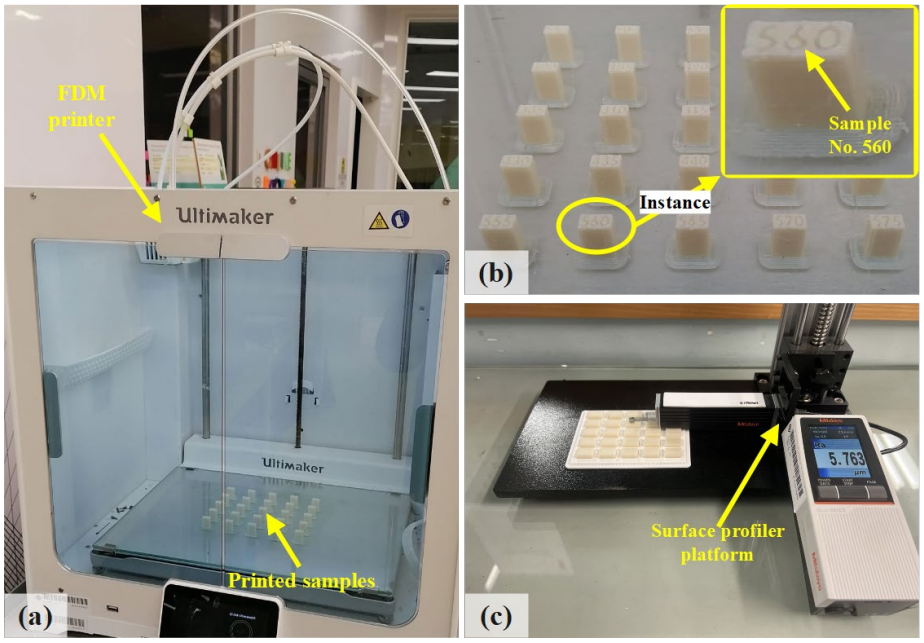


**Fig. 4.** Platform for 3D printing and measurement: (a) FDM printer with two extruders, (b) 3D-printed samples, (c) Surface profiler.

### *3.2. Constructing datasets of source and target domains*

#### *3.2.1. Dataset of the source domain*

Dataset construction is a critical step in AI-related studies as it directly impacts the final accuracy and effectiveness of intelligent models. When addressing issues related to 3D printing, datasets should include values associated with surface roughness and 3D printing parameters. This study employs the source domain dataset to train a FE based on the TL strategy. The dataset of the source domain is focused on the performance of line connection using the FDM process. This dataset is obtained from the experiment by Jiang *et al.* (Jiang et al., 2020), which contains 400 samples and is open for other researchers to use freely. The 3D printing parameters adopted in their

study are extrusion speed, printing speed, layer height, and line distance. The filament used in their experiment is also PLA, with a diameter of 1.75 mm.

The space gap is introduced to serve as an indicator to evaluate the impacts of printing parameters on the line connection performance. These samples are categorized into five groups in terms of the magnitude of the space gap. To eliminate the imbalance of the dataset in Ref. (Jiang et al., 2020), the SMOTE algorithm mentioned above is employed to preprocess the open-source dataset before feeding it into the 1DCNN model. To train a base model, eighty percent of the data from the source domain is allocated for training purposes, with the remaining data reserved for testing the model performance of predicting the space gap. More details of this dataset can also be found in Ref. (Jiang et al., 2020).

*3.2.2. Dataset of the target domain*

The dataset of the target domain concentrates on the relationship between 3D printing parameters and surface roughness. These samples are fabricated by FDM process-based 3D printing in our laboratory in accordance with Table 1. The target domain dataset is constructed by collecting surface roughness values which are then paired with corresponding 3D printing parameter configurations. A graphical representation of the original dataset of the target domain is shown in Fig. 5, in which the surface roughness distribution is plotted as a scattergram. According to the surface roughness of printed samples, the minimum value is 2.143 μm, and the maximum is 9.452 μm. Hence, thirteen customized categories are defined here, from C1 to C13. The

corresponding roughness scope of each category is enumerated in Table 2, with an interval of 0.6 μm.

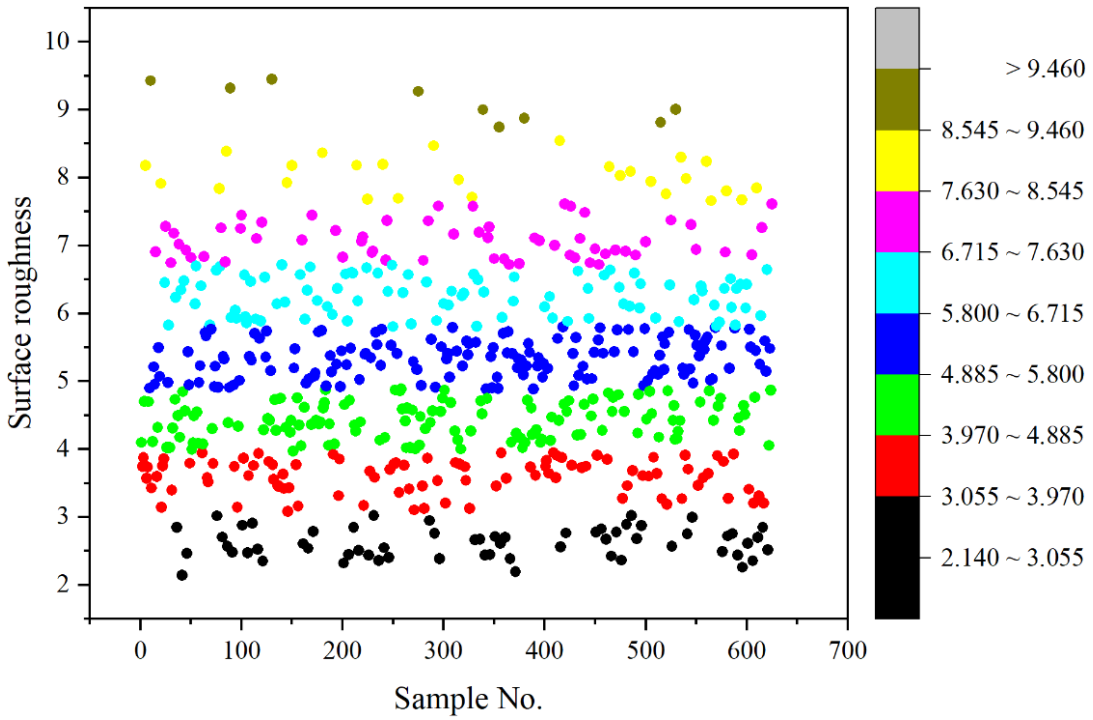


**Fig. 5.** Scattergram of surface roughness distribution.

The target domain dataset is also processed by the SMOTE algorithm to reduce any adverse effects arising from data imbalance. With these 3D printing parameters in the dataset, the knowledge derived from the source domain can be utilized to achieve accurate surface roughness prediction of FDM printed parts using an FE-GBDT classifier based on the TL strategy. Moreover, Table 3 is provided to intuitively display the discrepancies between the datasets of the source and target domains.

**Table 2**

Categories and surface roughness scopes for the dataset of the target domain.

| Category | C1 | C2 | C3 | … | C12 | C13 |
|---|---|---|---|---|---|---|
| Roughness scope | [2.0, 2.6) | [2.6, 3.2) | [3.2, 3.8) | … | [8.6, 9.2) | [9.2, 9.8) |

**Table 3**

Discrepancies between the two datasets of source and target domains.

| Domains | Specification | Quantity | Process parameters | Label (Indicator) |
|---|---|---|---|---|
| Source | Two lines | 400 | Extrusion speed<br>Line distance | Line gap |
| Target | Cuboid | 625 | Nozzle temp.<br>Material flow | Surface roughness |

## 4. Results and discussion

### *4.1. Building and evaluating the base model*

As described already, the hyperparameters of the base model are optimized with the RSCV in the defined parameters space. Five crucial parameters are selected for optimization, and the optimal hyperparameters are enumerated in Table 4. Then, the model with optimized hyperparameters is trained and tested on the dataset of the source

domain. Plots of the training history of the base model are illustrated in Fig. 6.

Fig. 6 illustrates the trends observed in the training and testing accuracy curves, which demonstrate a gradual ascent followed by a tendency to level off. This evidence substantiates the notion that the model has undergone continuous learning, resulting in significant improvements in its performance. In contrast, the training and testing loss curves exhibit a declining trend that stabilizes over time. This pattern implies that the model becomes increasingly accurate and efficient as the training progresses. These observations further support the claim that the model effectively learns and generalizes patterns without succumbing to overfitting on the training dataset. Consequently, these overall trends suggest that the model performance will continue to improve with further training, thereby rendering it suitable for practical applications in various fields.

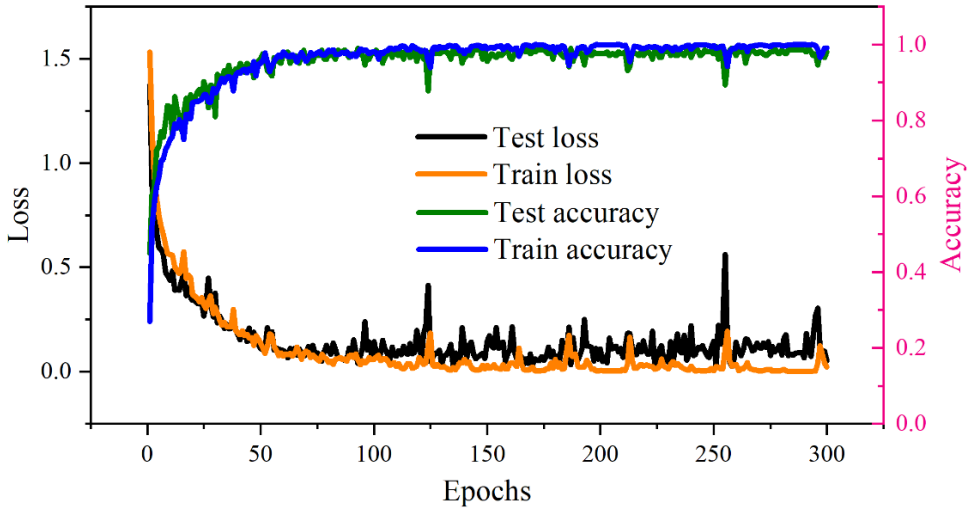


**Fig. 6.** Plots of the base model trained and tested on the dataset of the source domain.

Moreover, in order to assess the effectiveness of the base model, four performance metrics, namely Accuracy, Precision, Recall, and F1-score, have been adopted. The

scores for these metrics have been presented in Table 5. This table presents the indicator scores of evaluating the base model performance on the dataset from the source domain. The score for Accuracy is 0.9805, indicating a correct classification rate of 98.05% for the dataset instances. Moreover, the Precision score of 0.9811 suggests that 98.11% of the instances predicted as positive are correctly identified. The Recall score of 0.9805 further highlights the ability to capture 98.05% of the actual positive instances in the dataset. Lastly, the F1-score of 0.9805, which considers both precision and recall, comprehensively evaluates the overall performance. These consistently high scores across all indicators demonstrate robust and reliable performance on the dataset from the source domain.

The confusion matrix (CM) is commonly used to evaluate the performance of ML or DL models, especially in multi-class tasks. To visually represent the prediction results of the 1DCNN model on the testing set of the source domain, we present a diagram of CM to evaluate the performance of the base model, as diagramed in Figs. 7 (a) and (b). The two figures showcase the performance of the 1DCNN model on the testing set. Fig. 7 (b) is a normalized CM from Fig. 7 (a) to provide more comprehensive and intuitive prediction results. The diagonal elements of Fig. 7 (b) represent the accuracy for each class: 0.976 for class C1, 1 for class C2, C3, C4, and C5. These values demonstrate the high precision of our model in correctly predicting instances belonging to each class. Class C1 achieved a remarkable accuracy of 0.976, indicating the strong capability in accurately classifying instances from this category. Moreover, the perfect accuracies of 1.000 for classes C2, C3, C4, and C5 indicate that the model successfully

classified all instances from these classes without misclassifications. These results underscore the excellent performance of our classification model across all five labels. The detailed analysis using the CM diagram reveals insight into the efficiency of the base model. The prediction results suggest that the base model delivers significantly superior performance on the testing set.

**Table 4**

RSCV optimized hyperparameters for the base model using a dataset of source domain.

| Params. | Epochs | Batch | Filter#1 | Filter#2 | Filter#3 | Dropout rate#1 | Dropout rate#2 |
|---|---|---|---|---|---|---|---|
| Values | 300 | 32 | 32 | 64 | 128 | 0.30 | 0.38 |

**Table 5**

Indicator scores of base model performance on the dataset of the source domain.

| Indicators | Accuracy | Precision | Recall | F1-score |
|---|---|---|---|---|
| Scores | 0.9805 | 0.9811 | 0.9805 | 0.9805 |

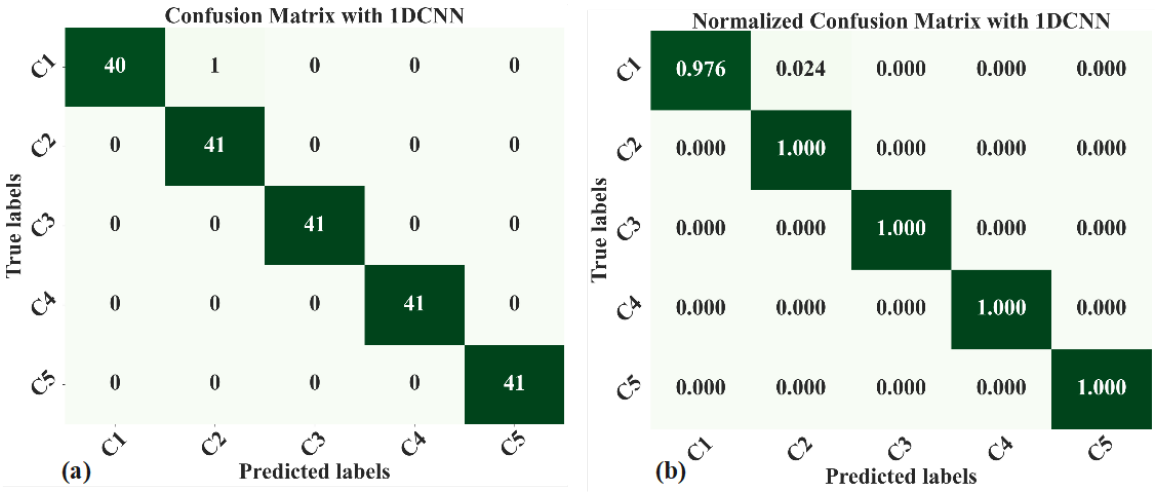


**Fig. 7.** Plots of surface quality prediction on the dataset of the source domain: (a) non-normalized CM, (b) normalized CM.

### *4.2. Evaluating effects of 3D printing parameters on surface quality*

#### *4.2.1. Confusion matrix on the dataset of target domain*

To visually display the results of FE-GBDT in the target domain, a CM is illustrated in Fig. 8. This figure is a normalized CM diagram that enables the comparisons among distinct class distributions based on diverse combinations of FDM process parameters. Similarly, the CM comprises different labels from C1 to C13, with the horizontal axis showing the predicted labels and the vertical axis representing the actual labels. The symbols from C1 to C13 have been elucidated in Table 2.

The diagonal elements of Fig. 8 represent the accuracy for each class. Specifically, some classes achieve perfect accuracies 1.0, indicating that the model accurately predicted all instances from these classes. For classes C3 and C4, an accuracy of 0.96 is obtained, suggesting a high precision in classifying instances belonging to these

categories. Notably, class C5 exhibited a slightly higher accuracy of 0.9900, emphasizing the model proficiency in correctly classifying instances within this particular category. The detailed analyses using the CM provide valuable insights into the performance of our classification model across the thirteen classes, positively contributing to the advancement of knowledge in intelligent model-empowered FDM printing.

The four indicators mentioned above are also employed to evaluate the performance of the FE-GBDT on the dataset of the target domain, as enumerated in Table 6. It can be seen from this table that the indicators for FE-GBDT evaluation are all over 0.9900, which proves the effectiveness and superior performance of predicting the surface quality on the target dataset. The accuracy score of 0.9918 reflects the overall correctness of the FE-GBDT predictions, indicating a high level of accuracy in classifying instances. The precision score of 0.9916 demonstrates the ability of FE-GBDT to identify positive instances among all predicted positives accurately. Similarly, the recall score, also 0.9916, showcases the effectiveness of FE-GBDT in correctly detecting positive instances from the total actual positives. Moreover, the F1-score of 0.9916 represents the harmonic mean of precision and recall, providing a comprehensive measure of the FE-GBDT performance. These results collectively indicate that the FE-GBDT model for class prediction accurately classifies instances.

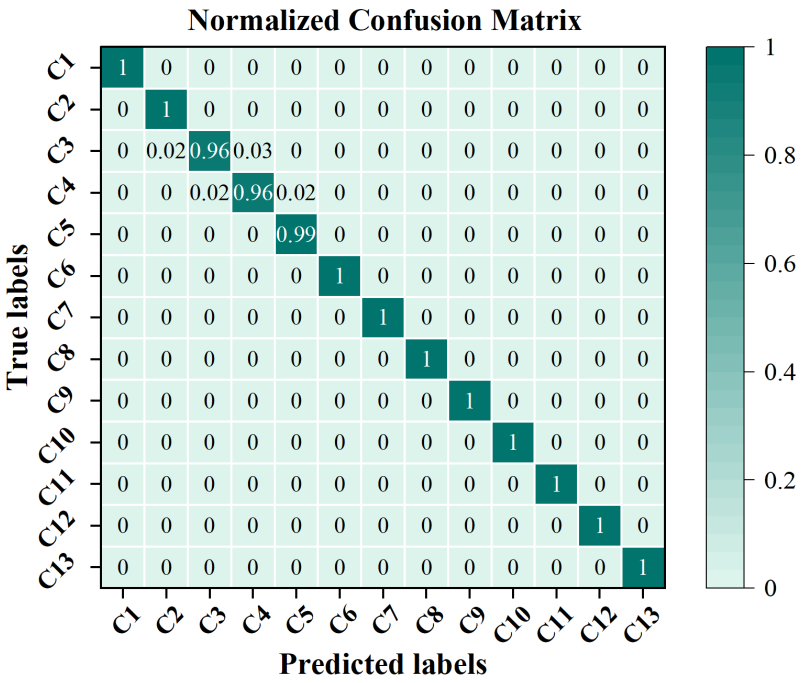


**Fig. 8.** Plot of normalized CM using FE-GBDT on the dataset of the target domain.

**Table 6**

Indicator scores of FE-GBDT approach on the dataset of the target domain.

| Indicators | Accuracy | Precision | Recall | F1-score |
|---|---|---|---|---|
| Scores | 0.9918 | 0.9916 | 0.9916 | 0.9916 |

*4.2.2. Comparison among FE-GBDT and conventional ML algorithms*

To evaluate the effectiveness of the proposed TL-enhanced FE-GBDT approach, exemplary algorithms in the ML community are introduced for comparison. The comparison is conducted on the target domain dataset. A bar graph of indicator scores depicting the performance of the proposed FE-GBDT approach and other ML algorithms, such as Support Vector Machine (SVM) and

Multinomial/Gaussian/Bernoulli Naïve Bayes (MNB/GNB/BNB), is diagramed in Fig. 9.

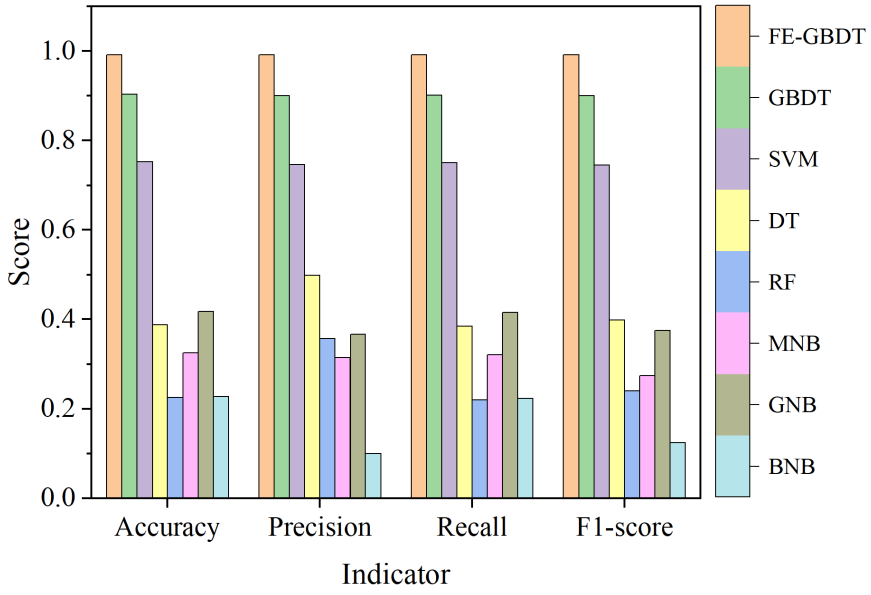


**Fig. 9.** Comparison among the FE-GBDT approach and exemplary ML algorithms.

From Fig. 9, it can be deduced that the height of a column chart is a visual representation that directly corresponds to the performance of a model. As the height of the columns increases, it indicates that larger values of the four indicators suggest better performance for the model being evaluated. By comparing the height between FE-GBDT and the conventional GBDT algorithm, it demonstrates that the developed approach in this study shows better performance when applied to the dataset of the target domain with the same GBDT configurations. To be specific, the FE-GBDT approach has an accuracy of approximately 9.5% higher than the conventional GBDT. The results from the analysis of Fig. 9 reveal compelling evidence that the proposed approach exhibits exceptional performance, as indicated by its notably greater column

height, surpassing the performance of the other mentioned ML algorithms.

*4.3. Contribution of process parameters to surface quality estimated with FE-GBDT*

As previously stated, the surface roughness of 3D-printed samples is significantly influenced by various printing parameter configurations. The proposed FE-GBDT approach in this study not only can achieve the prediction of surface quality based on various configurations of 3D printing parameters but also can be used to quantify the contribution of each parameter to the surface quality of the samples involved in the target domain. To visually present the results of quantifying the contribution of process parameters on surface quality, a bar graph of FI is plotted, as shown in Fig. 10.

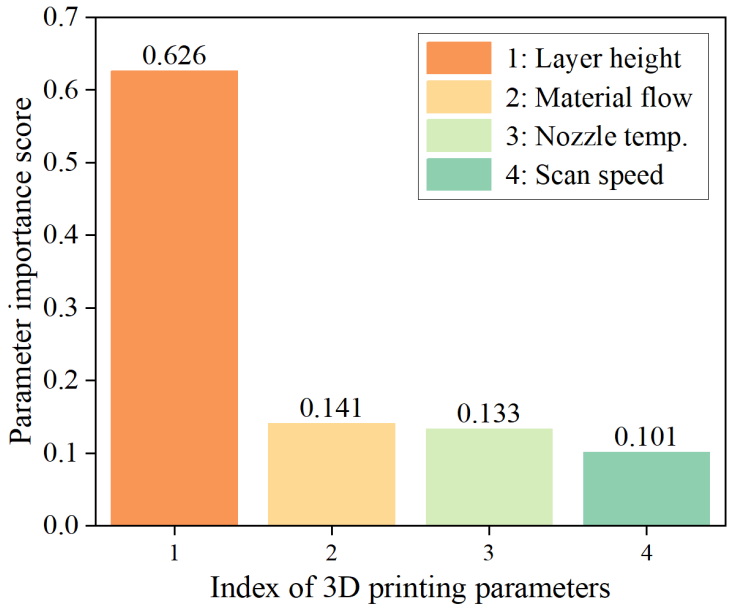


**Fig. 10.** Contribution of 3D printing parameters to surface quality.

The horizontal axis of Fig. 10 represents the index of 3D printing parameters, while the vertical axis indicates their importance score. The bar height in Fig. 10

corresponds to the degree of importance of each parameter. The results reveal that layer height has the most significant influence on the roughness of 3D-printed samples, contributing a score of 0.626. In contrast, the scan speed has the least effect on the surface quality of 3D-printed samples only with a FI score of 0.101. Contributions of the other two parameters are quantified as 0.133 and 0.141, respectively. These findings demonstrate that the proposed approach can effectively quantify the impact of process parameters on the surface quality of the 3D-printed samples.

## 5. Conclusions

This study introduces a newly-developed frame of the intelligent algorithm named FE-GBDT approach to assess the impact of 3D printing parameters on surface quality and quantify the contribution of each parameter. Surface roughness is adopted to characterize the surface quality of FDM-printed samples involved in this study. The SMOTE algorithm is deployed to eliminate the dataset imbalances. By using the source domain dataset, a 1DCNN model optimized by the RSCV algorithm is trained as the base model, which is employed for lowering the requirements for the quantity and quality of the dataset in the target domain, facilitating computation, and attaining superior performance with minimal retraining costs.

The results of this study demonstrate that the proposed FE-GBDT approach effectively uncovers the relationship between FDM process-based 3D printing parameters and the surface quality of final products by calculating the importance score of each printing parameter, with the maximum score of 0.626 for the layer height. The

FE-GBDT approach enhances the overall performance of quantitative evaluation, achieving high precision and accuracy over 0.9900 in the target domain. Furthermore, this approach quantifies each 3D printing parameter's contribution to surface quality, providing valuable insights for optimizing the printing processes. These findings hold potential implications for refining 3D printing process parameters and developing intelligent models for surface quality optimization.

Despite the merits of the proposed FE-GBDT approach, this study has certain limitations. Future research should encompass multiple source domains, larger-scale datasets, additional types of 3D printing process parameters, more complex structures, and cross-sectional designs.

**Acknowledgement**

Dr. Jianjian Zhu acknowledges the project supported by the Young Scientists Fund of the National Natural Science Foundation of China (Grant No. 52205171). Prof. Zhongqing Su acknowledges the support from the Hong Kong Research Grants Council via General Research Funds (Grant Nos. 15202820 and 15204419).

**CRediT authorship contribution statement**

**Jianjian Zhu:** Conceptualization, Data curation, Formal analysis, Investigation, Methodology, Software, Funding acquisition, Writing – original draft. **Zhongqing Su:** Funding acquisition, Methodology, Supervision, Writing – review & editing. **Qingqing Wang:** Investigation, Validation, Writing – review & editing. **Zifeng Lan:** Writing - review & editing. **Frankie Siu-fai Chan:** Investigation, Supervision. **Zhibin Han:**

Writing - review & editing. **Zhaokun Wang:** Writing - review & editing. **Sidney Wing-fai Wong:** Project administration. **Andy Chi-fung Ngan:** Investigation, Validation.

## Declaration of competing interest

The authors declare that they have no known competing financial interests or personal relationships that could have appeared to influence the work reported in this paper.

## Data availability

Data will be made available on request.

## References


Agarwal, N., Sondhi, A., Chopra, K., & Singh, G. (2021). Transfer Learning: Survey and Classification. In S. Tiwari, M. C. Trivedi, K. K. Mishra, A. K. Misra, K. K. Kumar, & E. Suryani (Eds.), *Smart Innovations in Communication and Computational Sciences* (25; pp. 145–155). Springer. https://doi.org/10.1007/978-981-15-5345-5_13

Altan, M., Eryildiz, M., Gumus, B., & Kahraman, Y. (2018). Effects of process parameters on the quality of PLA products fabricated by fused deposition modeling (FDM): Surface roughness and tensile strength. *Materials Testing*, *60*(5), 471–477. https://doi.org/10.3139/120.111178

Andradóttir, S. (2006). Chapter 20 An Overview of Simulation Optimization via Random Search. In S. G. Henderson & B. L. Nelson (Eds.), *Handbooks in*

*Operations Research and Management Science* (Vol. 13, pp. 617–631). Elsevier. https://doi.org/10.1016/S0927-0507(06)13020-0

Andradóttir, S. (2015). A Review of Random Search Methods. In M. C. Fu (Ed.), *Handbook of Simulation Optimization* (pp. 277–292). Springer. https://doi.org/10.1007/978-1-4939-1384-8_10

Barrios, J. M., & Romero, P. E. (2019). Decision Tree Methods for Predicting Surface Roughness in Fused Deposition Modeling Parts. *Materials*, *12*(16), Article 16. https://doi.org/10.3390/ma12162574

Blagus, R., & Lusa, L. (2013). SMOTE for high-dimensional class-imbalanced data. *BMC Bioinformatics*, *14*(1), 106. https://doi.org/10.1186/1471-2105-14-106

Boschetto, A., Giordano, V., & Veniali, F. (2013). Surface roughness prediction in fused deposition modelling by neural networks. *The International Journal of Advanced Manufacturing Technology*, *67*(9), 2727–2742. https://doi.org/10.1007/s00170-012-4687-x

Cerro, A., Romero, P. E., Yiğit, O., & Bustillo, A. (2021). Use of machine learning algorithms for surface roughness prediction of printed parts in polyvinyl butyral via fused deposition modeling. *The International Journal of Advanced Manufacturing Technology*, *115*(7), 2465–2475. https://doi.org/10.1007/s00170-021-07300-2

Charalampous, P., Kladovasilakis, N., Kostavelis, I., Tsongas, K., Tzetzis, D., & Tzovaras, D. (2022). Machine Learning-Based Mechanical Behavior Optimization of 3D Print Constructs Manufactured Via the FFF Process. *Journal of Materials*

*Engineering and Performance*, *31*(6), 4697–4706. https://doi.org/10.1007/s11665-021-06535-0

Chawla, N. V., Bowyer, K. W., Hall, L. O., & Kegelmeyer, W. P. (2002a). SMOTE: Synthetic Minority Over-sampling Technique. *Journal of Artificial Intelligence Research*, *16*, 321–357. https://doi.org/10.1613/jair.953

Chawla, N. V., Bowyer, K. W., Hall, L. O., & Kegelmeyer, W. P. (2002b). SMOTE: Synthetic Minority Over-sampling Technique. *Journal of Artificial Intelligence Research*, *16*, 321–357. https://doi.org/10.1613/jair.953

Dey, A., & Yodo, N. (2019). A Systematic Survey of FDM Process Parameter Optimization and Their Influence on Part Characteristics. *Journal of Manufacturing and Materials Processing*, *3*(3), Article 3. https://doi.org/10.3390/jmmp3030064

Fernandez, A., Garcia, S., Herrera, F., & Chawla, N. V. (2018). SMOTE for Learning from Imbalanced Data: Progress and Challenges, Marking the 15-year Anniversary. *Journal of Artificial Intelligence Research*, *61*, 863–905. Q2. https://doi.org/10.1613/jair.1.11192

Hooda, N., Chohan, J. S., Gupta, R., & Kumar, R. (2021). Deposition angle prediction of Fused Deposition Modeling process using ensemble machine learning. *ISA Transactions*, *116*, 121–128. https://doi.org/10.1016/j.isatra.2021.01.035

Jaisingh Sheoran, A., & Kumar, H. (2020). Fused Deposition modeling process parameters optimization and effect on mechanical properties and part quality: Review and reflection on present research. *Materials Today: Proceedings*, *21*,

1659–1672. https://doi.org/10.1016/j.matpr.2019.11.296

Jiang, J., Yu, C., Xu, X., Ma, Y., Liu, J., Jiang, J., Yu, C., Xu, X., Ma, Y., & Liu, J. (2020). Achieving better connections between deposited lines in additive manufacturing via machine learning. *Mathematical Biosciences and Engineering*, *17*(4), Article mbe-17-04-191. Q3. https://doi.org/10.3934/mbe.2020191

Jin, Z., Zhang, Z., & Gu, G. X. (2019). Autonomous in-situ correction of fused deposition modeling printers using computer vision and deep learning. *Manufacturing Letters*, *22*, 11–15. https://doi.org/10.1016/j.mfglet.2019.09.005

Jindal, S., Manzoor, F., Haslam, N., & Mancuso, E. (2021). 3D printed composite materials for craniofacial implants: Current concepts, challenges and future directions. *The International Journal of Advanced Manufacturing Technology*, *112*(3), 635–653. https://doi.org/10.1007/s00170-020-06397-1

Kam, M., İpekçi, A., & Şengül, Ö. (2023). Investigation of the effect of FDM process parameters on mechanical properties of 3D printed PA12 samples using Taguchi method. *Journal of Thermoplastic Composite Materials*, *36*(1), 307–325. https://doi.org/10.1177/08927057211006459

Li, N., Huang, S., Zhang, G., Qin, R., Liu, W., Xiong, H., Shi, G., & Blackburn, J. (2019). Progress in additive manufacturing on new materials: A review. *Journal of Materials Science & Technology*, *35*(2), 242–269. https://doi.org/10.1016/j.jmst.2018.09.002

Li, Z., Zhang, Z., Shi, J., & Wu, D. (2019). Prediction of surface roughness in extrusion-based additive manufacturing with machine learning. *Robotics and Computer-*

*Integrated Manufacturing*, *57*, 488–495. https://doi.org/10.1016/j.rcim.2019.01.004

Liang, W., Luo, S., Zhao, G., & Wu, H. (2020). Predicting Hard Rock Pillar Stability Using GBDT, XGBoost, and LightGBM Algorithms. *Mathematics*, *8*(5), 765. https://doi.org/10.3390/math8050765

Liashchynskyi, P., & Liashchynskyi, P. (2019). *Grid Search, Random Search, Genetic Algorithm: A Big Comparison for NAS* (arXiv:1912.06059). arXiv. https://doi.org/10.48550/arXiv.1912.06059

Ngo, T. D., Kashani, A., Imbalzano, G., Nguyen, K. T. Q., & Hui, D. (2018). Additive manufacturing (3D printing): A review of materials, methods, applications and challenges. *Composites Part B: Engineering*, *143*, 172–196. https://doi.org/10.1016/j.compositesb.2018.02.012

Pérez, M., Medina-Sánchez, G., García-Collado, A., Gupta, M., & Carou, D. (2018). Surface Quality Enhancement of Fused Deposition Modeling (FDM) Printed Samples Based on the Selection of Critical Printing Parameters. *Materials*, *11*(8), Article 8. https://doi.org/10.3390/ma11081382

Radhwan, H., Shayfull, Z., Farizuan, M. R., Effendi, M. S. M., & Irfan, A. R. (2019). Optimization parameter effects on the quality surface finish of the three-dimensional printing (3D-printing) fused deposition modeling (FDM) using RSM. *AIP Conference Proceedings*, *2129*(1), 020155. https://doi.org/10.1063/1.5118163

Rajamani, D., Balasubramanian, E., & Yang, L.-J. (2022). Enhancing the Surface Quality of FDM Processed Flapping Wing Micro Mechanism Assembly through

RSM–TOPSIS Hybrid Approach. *Processes*, *10*(11), Article 11. https://doi.org/10.3390/pr10112457

Rao, H., Shi, X., Rodrigue, A. K., Feng, J., Xia, Y., Elhoseny, M., Yuan, X., & Gu, L. (2019). Feature selection based on artificial bee colony and gradient boosting decision tree. *Applied Soft Computing*, *74*, 634–642. https://doi.org/10.1016/j.asoc.2018.10.036

Tan, C., Sun, F., Kong, T., Zhang, W., Yang, C., & Liu, C. (2018). A Survey on Deep Transfer Learning. In V. Kůrková, Y. Manolopoulos, B. Hammer, L. Iliadis, & I. Maglogiannis (Eds.), *Artificial Neural Networks and Machine Learning – ICANN 2018* (1688 ; pp. 270–279). Springer International Publishing. https://doi.org/10.1007/978-3-030-01424-7_27

Weiss, K., Khoshgoftaar, T. M., & Wang, D. (2016). A survey of transfer learning. *Journal of Big Data*, *3*(1), 9. https://doi.org/10.1186/s40537-016-0043-6

Wu, D., Wei, Y., & Terpenny, J. (2019). Predictive modelling of surface roughness in fused deposition modelling using data fusion. *International Journal of Production Research*, *57*(12), 3992–4006. https://doi.org/10.1080/00207543.2018.1505058

Yang, L., Li, S., Li, Y., Yang, M., & Yuan, Q. (2019). Experimental Investigations for Optimizing the Extrusion Parameters on FDM PLA Printed Parts. *Journal of Materials Engineering and Performance*, *28*(1), 169–182. https://doi.org/10.1007/s11665-018-3784-x

Zhang, J., Wang, P., & Gao, R. X. (2019). Deep learning-based tensile strength prediction in fused deposition modeling. *Computers in Industry*, *107*, 11–21.

https://doi.org/10.1016/j.compind.2019.01.011

Zhang, Z., & Jung, C. (2021). GBDT-MO: Gradient-Boosted Decision Trees for Multiple Outputs. *IEEE Transactions on Neural Networks and Learning Systems*, *32*(7), 3156–3167. https://doi.org/10.1109/TNNLS.2020.3009776

Zhuang, F., Qi, Z., Duan, K., Xi, D., Zhu, Y., Zhu, H., Xiong, H., & He, Q. (2021). A Comprehensive Survey on Transfer Learning. *Proceedings of the IEEE*, *109*(1), 43–76. https://doi.org/10.1109/JPROC.2020.3004555